

Doubly-Fed Induction Generator Wind Turbine Model for Fault Ride-Through Investigation

Yutana Chongjarearn¹, Non-member

ABSTRACT

The paper presents an investigation into the behavior of a grid-connected, wind turbine driven Doubly-Fed Induction Generator (DFIG) during Grid faults which are represented by a voltage dip on all three phases of the voltage supply. Stator-voltage-oriented vector control is used to decouple the active and reactive power generated by the machine. The dynamic DFIG model is used to simulate the behaviour of the wind turbine generator during both normal and fault conditions. Simulation and experiment results are shown in a very good agreement. Further the model can be used to investigate Fault ride-through performance of the DFIG.

Keywords: DFIGt, Fault ride-through, Doubly-Fed Induction Generator

1. INTRODUCTION

The Doubly-Fed Induction Generator is widely used for large grid-connected, variable-speed wind turbines. Variable speed wind turbines offer a number of advantages [1] when compared with fixed-speed turbines, including operation over a wide range of wind velocities, independent control of active and reactive power, reduced flicker and lower acoustic noise levels.

As the amount of installed wind power increases, it is becoming increasingly more important that turbine generators remain connected and support the grid transmission network during transient system disturbances- so-called fault ride-through (FRT), as specified by various national grid codes [2].

To study the fault ride-through capability of the DFIG, an accurate model of the system is needed; this must include details of mechanical, electrical and control systems' behavior if it is to accurately predict the fault ride through performance of the generator.

In this paper, a new model for a vector controlled doubly-fed induction generator is developed to investigate drive fault through characteristics, allowing for the switching effects of all IGBTs and anti-parallel diodes. The model is used to study the fault ride

through performance of the DFIG in accordance with the transmission system grid codes.

The paper is organized as follows. First, the system modelling is reviewed and discussed. Then, simulation results of two fault scenarios is obtained and compared with measurements. Finally, the model will be used to investigate the FRT capability of the DFIG.

2. DYNAMIC MODEL OF A DOUBLY FED INDUCTION GENERATOR

A doubly-fed induction generator (DFIG) is composed of a three-phase wound rotor induction machine with a supply connected stator winding and a rotor winding fed through a PWM controlled converter via slip rings (Fig. 1).

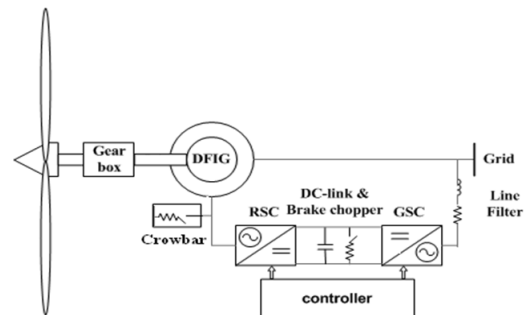


Fig.1: A diagram of a DFIG wind turbine.

Two three-phase, voltage source converters are employed in the scheme: a rotor side converter (RSC) and a grid side converter (GSC) connected back-to-back in a dc link arrangement and controlled using vector control methods [1-3]. In this paper, a stator-voltage-oriented, vector control DFIG model capable of modeling the switching of the power electronic devices employed in the two IGBT converters is developed using Matlab/Simulink.

A. Drive train and wind turbine

A two-mass representation of the drive train has been used in many literatures [4] which is suitable to model the mechanical part for investigating behavior of DFIG under fault conditions.

B. Power converters

Either RSC or GSC is modeled with six IGBTs and anti-parallel diodes connected back to back. Either the Diode or IGBT is simulated by a resistor, inductor and DC voltage source connected in series with a

Manuscript received on July 15, 2012 ; revised on October 12, 2012.

¹ The author is with Department of Electrical Engineering, Faculty of Engineering Dhurakij Pundit University, Bangkok, Thailand., E-mail: yutana.cho@dpu.ac.th

switch. The Diode switching operation is controlled by the anode-cathode voltage and current while IGBTs switching operation is controlled by the gate signal, the collector-emitter voltage and current which each model can be found in MATLAB/Simulink (sim-power toolbox). Switching of these IGBTs is operated with the Pulse-Width Modulation Techniques (PWM) as shown in vector control scheme. In this control scheme, the task of RSC is to decouple control of the stator active and reactive power of the DFIG while the GSC has to keep the DC-link voltage constant at a reference demand regardless of the magnitude and direction of the rotor power. Both converters are normally set to operate at unity power factor using stator voltage-oriented vector control. The converters are controlled independently with a switching frequency of 5 kHz, according to a laboratory test.

C. DFIG

The dynamic model of DFIG is the space vector representation of electrical quantities with the state equation (1)-(2) for stator and rotor side voltage [3].

$$\bar{v}_s = R_s \bar{i}_s + \frac{1}{\omega_b} \frac{d\bar{\lambda}_s}{dt} + \omega_e M \bar{\lambda}_s \quad (1)$$

$$\bar{v}_r = R_r \bar{i}_r + \frac{1}{\omega_b} \frac{d\bar{\lambda}_r}{dt} + (\omega_e - \omega_r) M \bar{\lambda}_r \quad (2)$$

Where M represents a space rotator namely $M = [0 \ -1; 1 \ 0]$.

Stator and rotor flux linkage can be given by equation (3)-(4).

$$\bar{\lambda}_s = L_m \bar{i}_r + L_s \bar{i}_s \quad (3)$$

$$\bar{\lambda}_r = L_m \bar{i}_s + L_r \bar{i}_r \quad (4)$$

D. DFIG Power and Current Control

From the equation (1)-(2), all quantities are decomposed into the d-q frame using stator voltage-oriented techniques. All voltage and currents in d-q frame can be substituted in a power flow equation as mentioned in [3]. Therefore, the stator active (P_s) and reactive (Q_s) power generated by the DFIG can be expressed in equation (5)-(6).

$$P_s = v_{sd} i_{sd} = v_{sd} \left(-\frac{L_m i_{rd}}{L_s} \right) \quad (5)$$

where $i_{sd} = -L_m i_{rd} / L_s$

$$Q_s = -v_{sd} i_{sq} = -v_{sd} \left(\frac{\lambda_{sq}}{L_s} - \frac{L_m i_{rq}}{L_s} \right) \quad (6)$$

where $i_{sq} = (\lambda_{sq} - L_m i_{rq}) / L_s$

Since the q-axis flux linkage component (λ_{sq}), the stator self inductance (L_s), the mutual inductance (L_m) and the d-axis stator voltage component (V_{sd}) are constant, the DFIG active power and reactive power are independently controlled by the d-axis rotor current component (i_{rd}) and the q-axis rotor current component (i_{rq}), respectively.

In RSC power controller, a typical power-speed curve is used to define the reference output power for the controller according to the Turbine Characteristic in which to track the maximum power at each wind and generator speed. The reference rotor currents for control of active and reactive powers can be expressed as

$$i_{rdref} = PI(P_{ref} - P_{meas}), i_{rqref} = PI(Q_{ref} - Q_{meas}) \quad (7)$$

Where i_{rdref} and i_{rqref} are references for RSC power control and PI is the proportional and integral gain.

From the equation (2), the rotor side voltages can be rewritten in the d-q-axis components.

$$\begin{aligned} v_{rd} &= R_r i_{rd} - (\omega_e - \omega_r) \sigma L_r i_{rq} - (\omega_e - \omega_r) \frac{L_m}{L_s} \lambda_{sq} + \frac{1}{\omega_b} \sigma L_r \frac{dt_{rd}}{dt} \\ v_{rq} &= R_r i_{rq} + (\omega_e - \omega_r) \sigma L_r i_{rd} + \frac{1}{\omega_b} \left(\sigma L_r \frac{di_{rq}}{dt} + \frac{L_m}{L_s} \frac{d\lambda_{sq}}{dt} \right) \end{aligned} \quad (8)$$

Where $\sigma = 1 - L_m^2 / L_r L_s$.

There are rotational emf term and transformer emf term (the derivative of flux) in each component. Since the operating slip range of DFIG is limited, the effects of the former term are very small and also the stator flux is assumed constant. Therefore, the reference rotor voltages for control of active and reactive powers can be expressed as

$$\begin{aligned} v_{rdref} &= PI(i_{rdref} - i_{rd}) \\ v_{rqref} &= PI(i_{rqref} - i_{rq}) \end{aligned} \quad (9)$$

Where v_{rdref} , v_{rqref} are references for RSC current control and PI is the proportional and integral gain.

In GSC controller, similar to RSC, all quantities are decomposed into the d-q frame using stator voltage-oriented techniques. All voltages and currents between grid and GSC converter can be expressed in d-q frame as

$$\begin{aligned} v_{cd} &= R i_{cd} + L \frac{di_{cd}}{dt} - \omega_e L i_{cq} + v_{cd1} \\ v_{cq} &= R i_{cq} + L \frac{di_{cq}}{dt} - \omega_e L i_{cd} + v_{cq1} \end{aligned} \quad (10)$$

Where R, L is a line side filter between Grid and GSC.

The active (P_c) and reactive (Q_c) power as mentioned in [3] can be expressed in equation (11)-(12).

$$P_c = v_{cd} i_{cd} \quad (11)$$

$$Q_c = -v_{cd}i_{cq} \quad (12)$$

As shown in equations, the active and reactive power is proportional to the d-axis and q-axis converter current component (i_{cdq}).

In DC-Link voltage control, the energy stored in the DC-link capacitor is considered as $cv_{dc}^2/2$. The time derivative of the energy is equal to the sum of GSC and RSC power. Hence the DC-Link equations are obtained as:

$$\frac{1}{2}c \frac{dv_{dc}^2}{dt} = P_{GSC} - P_{RSC} \quad (13)$$

Where $PGSC = vcdicd$, $PRSC = vrdird + vrqirq$ and $icrsc = Pr/vdc$, $icgsc = Pc/vdc$. Hence,

$$\frac{1}{2}C \frac{dv_{dc}}{dt} = i_{cgsc} - i_{crsc} \quad (14)$$

From equation (13) and (14), it can be concluded that the DC-link voltage can be controlled using the GSC current in the d-axis component while the reactive power is controlled using the GSC current in the q-axis component.

From equation (10), it can be rearranged as

$$\begin{aligned} v_{cd1} &= -\left(Ri_{cd} + L\frac{di_{cd}}{dt}\right) + \omega_e Li_{cq} + v_{cd} \\ v_{cq1} &= -\left(Ri_{cd} + L\frac{di_{cq}}{dt}\right) - \omega_e Li_{cd} \end{aligned} \quad (15)$$

Therefore, the reference voltages for GSC can be expressed as:

$$\begin{aligned} v_{cdref} &= -PI(i_{cdref} - i_{cd}) + feedforward_term \\ v_{cqref} &= -PI(i_{cqref} - i_{cq}) + feedforward_term \end{aligned} \quad (16)$$

Where PI is the proportional and integral gain and v_{cdref} , v_{cqref} are references for GSC current control.

In order to offer preferable dynamic response to grid voltage dips, the feed-forward term is estimated to the stator voltage [5].

To generate 3-phase PWM signals to drive the converters connected to the rotor and grid sides, the voltage demand needs to be scaled by using the factor, K_1 and DC-link voltage, v_{dc} to produce the modulation factor, m_r for RSC and m_c for GSC. The modulation factor can be given by

$$m_r = K1 * v_{rdqref}/v_{dc} \quad (17)$$

$$m_c = K1 * v_{cdqref}/v_{dc} \quad (18)$$

Where $K1 = ((2\sqrt{2}) * v_{rac} / \sqrt{3})$.

A diagram of vector control scheme for RSC and GSC is shown in Fig. 2.

3. MODEL VALIDATION

The model is validated using the laboratory DFIG test rig operating at speed of 1.12 p.u. (12% above synchronous) and generating 5kW (0.67 pu) power at unity power factor.

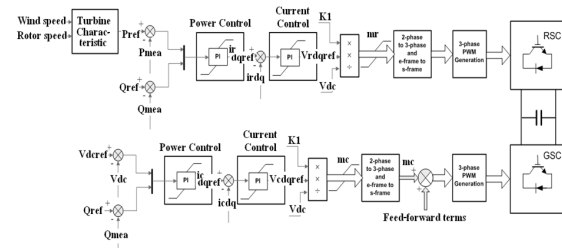


Fig.2: Vector control scheme for RSC and GSC.

Two fault scenarios regarding the FRT GB grid code are investigated in the paper as concluded in Table 1.

Table 1: Two cases of the fault scenarios.

Case	Fault Voltage (pu)	Fault duration (sec)	Voltage Recovery (pu)
1	0	0.14	0.9
2	0.15	0.50	0.9

NB. All fault scenarios start at time of 1 sec.

The applied fault is a 3-phase grid voltage dip from a normal voltage (1 pu) to a fault voltage of 0 and 0.15 pu, respectively. All fault scenarios initiate at time of 1 sec and clear at time of 1.14 and 1.5 sec, respectively. After that case of 0.15 pu fault voltage will be investigated for the FRT capability of the DFIG.

4. RESULTS AND DISCUSSION

The resulting simulated and measured stator currents, rotor currents, active and reactive powers are shown in Fig. 3 and 4. Comparisons between simulation and experiment peak stator and rotor currents result in the following conclusions: During fault initiation (at time of 1sec) and clearance (at time of 1.14 for case1 and 1.5 sec for case 2, respectively), both stator and rotor currents can spike and reach the value of 60A (4pu) and 40A (4pu), respectively. The spike at the rotor side can damage the power electronics devices (IGBTs or Diodes) inside the RSC converter if there has no protection.

Both after fault initiation period of 0.05 sec and after fault clearance time of 0.03 sec, fault stator and rotor currents, active and reactive powers between simulation and experiment are shown in a very good agreement (see Fig. 3 and 4).

After model validation for two cases, the case of 0.15 pu fault voltage is used to investigate for the FRT capability of the DFIG which included a crowbar (between RSC and rotor of DFIG) and DC chopper (across DC link between RSC and GSC) in the model. The crowbar is set to operate at absolute peak rotor current of 2 pu and the DC chopper is set to switch on and off at DC voltage of 1.08 pu and 1.06 pu, respectively. The simulation results are shown in Fig. 5. The results show that stator currents, rotor currents and active and reactive powers are similar to case 2 which doesn't have a crowbar and chopper protections but in the FRT protection case the RSC currents are different because the crowbar protection can protect the converter after peak currents reach 2 pu while in case 2 (no crowbar and DC chopper protection) the converter could be damaged. For DC link voltage, it can be increased until capacitor broken if no DC chopper. Therefore, as part of FRT capability of the DFIG, the crowbar is used to protect the converter while DC chopper helps the system to release an energy across the DC link and also prevent capacitor breakage.

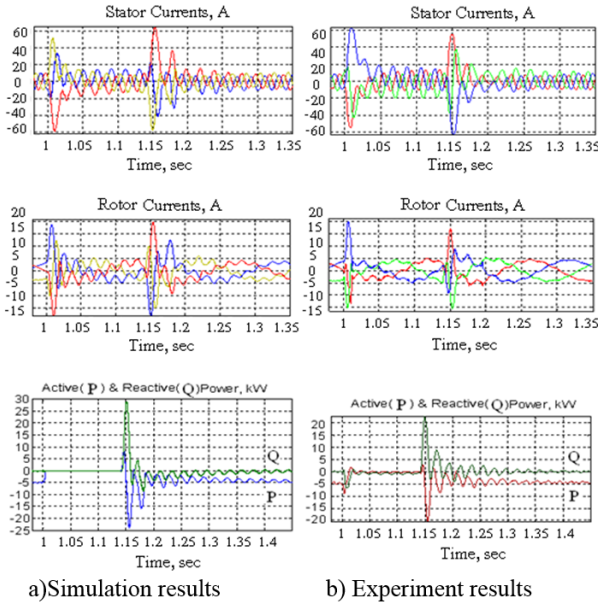


Fig.3: Simulation (left side) and Experiment (right side) Wave forms for three phase faults of case 1(0.1pu).

5. CONCLUSIONS

A new model for a vector controlled doubly-fed induction generator is developed to investigate drive fault ride through characteristics, allowing for switch-

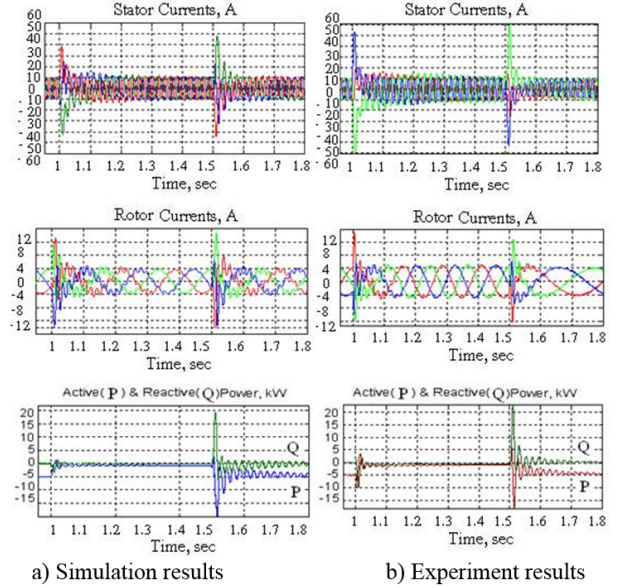


Fig.4: Simulation (left side) and Experiment (right side) Wave forms for three phase faults of Case 2 (0.15 pu).

ing effects of all rotor and supply side converter devices. Simulations are compared with measurements using a 7.5 kW laboratory DFIG operating under fault conditions, showing a very good agreement. The model can be used to investigate the fault ride through performance of the DFIG in accordance with the transmission system grid codes.

6. ACKNOWLEDGMENT

The author would like to thank my supervisors, Dr. Bashar Zahawi and Dr. David Atkinson during doing this research at Power electronics, Drives and Machines Research Lab, Newcastle University, UK

References

- [1] S. Muller, M. Deicke, and R. W. De Doncker, "Doubly fed induction generator systems for wind turbines," in *IEEE Industry Applications Magazine.*, vol. 8, 2002, pp. 26-33.
- [2] M. Tsili, S. Papathanassiou, G. Georgantzis, and G. Antonopoulos, "Grid code requirements for large wind farms: A review of technical regulations and available wind turbine technologies," in *Proc. EWE'08*, Brussels 2008., pp. 1-11, 2008.
- [3] P. Kundur, N. J. Balu, and M. G. Lauby, *Power system stability and control.*, New York: McGraw-Hill, 1994.
- [4] T. Ackermann, *Wind power in power systems.* Chichester, West Sussex, England: John Wiley, 2005.
- [5] G. Pannell, "Grid Fault Ride Through for Wind Turbine Doubly-Fed Induction Generators," in *IEEE Transactions on Energy Conversion*, vol. 22, no. 3, pp. 681-688, 2007.

tors," *EngD Thesis*, University of Newcastle upon Tyne, 2008.

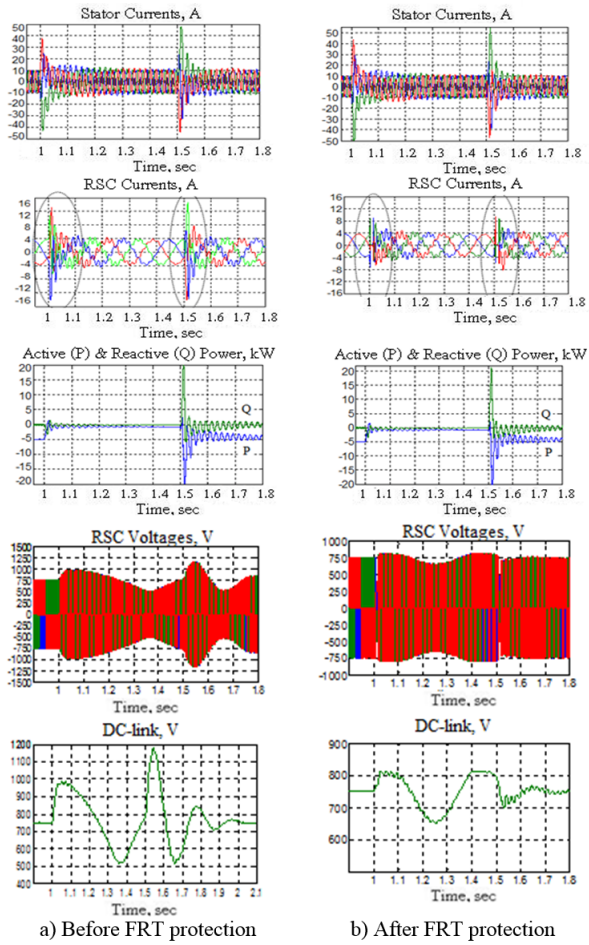


Fig.5: Simulated comparisons between before and after FRT protection.



Yutana Chongjarearn received B.Eng and M.Eng degrees from Kasetsart University, Thailand and currently a PhD (Integrated) candidate at Newcastle University, UK. He also works as a lecturer in department of Electrical Engineering, Dhurakij Pundit University. His research interests are electrical machines and drives, power electronics application for renewable energy and power system analysis.